Journal of Power Sources 253 (2014) 404–411

Contents lists available at ScienceDirect

Journal of Power Sources

journal homepage: www.elsevier.com/locate/jpowsour

Optimization of Multi-Walled Carbon Nanotube based CF_x electrodes for improved primary and secondary battery performances

Ruwantha Jayasinghe [a], Arjun Kumar Thapa [b], Ruchira R. Dharmasena [a], Tu Quang Nguyen [b], Bhabendra K. Pradhan [c], Hem Sharma Paudel [d], Jacek B. Jasinski [b], Andriy Sherehiy [a,b], Masaki Yoshio [e], G.U. Sumanasekera [a,b,*]

[a] Department of Physics & Astronomy, University of Louisville, Louisville, KY 40292, USA
[b] Conn Center for Renewable Energy Research, University of Louisville, Louisville, KY 40292, USA
[c] NanoHoldings LLC., Rowayton, CT 06853, USA
[d] Department of English, University of Louisville, Louisville, KY 40292, USA
[e] Advanced Research Center, Saga University, 1341 Yoga-Machi, Saga 840-0047, Japan

HIGHLIGHTS

- In this study, fluorination was performed on MWCNTs using plasma fluorination.
- Fluorinated MWCNT was used as cathode for CF_x primary battery and anode for Li-ion battery.
- Fully fluorinated MWCNT shows the discharge capacity of 815 mAh g^{-1} for CF_x primary battery.
- Mild fluorinated MWCNT anode electrode shows the highest capacity of 713 mAh g^{-1}.

ARTICLE INFO

Article history:
Received 16 September 2013
Received in revised form
3 December 2013
Accepted 16 December 2013
Available online 25 December 2013

Keywords:
MWCNT
Plasma fluorination
Primary battery
Secondary battery

ABSTRACT

Multi-walled carbon nanotubes synthesized using fluidized bed chemical vapor deposition technique were fluorinated sequentially to prepare a series of CF_x battery electrodes. Primary battery performance was tested using CF_x as a cathode against Li. Fully fluorinated MWNTs showed capacity exceeding 815 mAh g^{-1} while partially fluorinated samples showed systematically lowered capacity with decreasing x (in CF_x). However, fully fluorinated MWCNTs showed distinctly low rechargeable capacity compared to the subfluorinated samples when used as an anode against Li. Mildly fluorinated MWNTs show high capacity and better stability during charge–discharge cycles. High concentrations of fluorine seem to affect capacity retention due to the increased defect densities and reduced electronic conduction. These defects of nanotubes will provide additional pathways for lithium ions to diffuse within the core of the fluorinated structure and to access the electrochemically active C–F sites. XRD, XPS, and Raman spectroscopy were utilized to characterize the samples. Finally the electrochemical performance of fluorinated MWNTs was compared with that of Natural Chinese Graphite (NCG).

1. Introduction

In spite of current interests in Li-ion technology for secondary batteries, there is an eminent need for primary batteries with optimal energy and power densities. Lithium/Carbon fluoride (CF_x) primary batteries are very attractive because they offer very high-energy density, long-storage life, very good safety record, a wide temperature operating range, and very low self-discharge [1]. These batteries are found in a wide range of applications in military [2], aerospace [3], electronics [4], and medical industry [5,6]. Tunability of the properties of cathode in Li/CF_x batteries allows cell's fundamental properties to be fine-tuned for better performance. Recent innovations in the formation of nanostructured carbon fluoride powders offer the potential to eliminate traditional shortcomings in CF_x batteries. The most significant advancement found in these new Lithium/CF_x batteries is the ability to tune the cathode to meet the specific requirements. By altering how fluorine is introduced into the carbon structure at the atomic level during the synthesis process, the batteries fundamental properties can be changed to achieve higher energy or power densities.

* Corresponding author. Conn Center for Renewable Energy Research, University of Louisville, Louisville, KY 40292, USA. Tel.: +1 502 852 1558; fax: +1 502 852 0742.
E-mail addresses: gamini.sumanasekera@louisville.edu, akthap01@louisville.edu (G.U. Sumanasekera).

0378-7753/$ – see front matter © 2013 Elsevier B.V. All rights reserved.
http://dx.doi.org/10.1016/j.jpowsour.2013.12.076

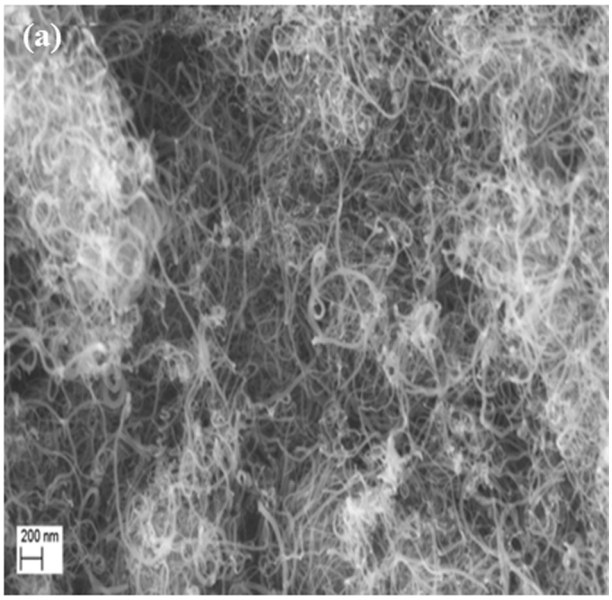

Fig. 1. SEM image of MWCNTs.

Traditional CF_x based cathode materials are formed by high-temperature intercalation of fluorine gas into graphite powder, [7] paving the way for primary batteries with high energy density (250 Wh kg^{-1}) and 7-year shelf life. Key medical applications include: drug infusion pumps, neuro-stimulators or implanted pulse generators, pacemakers, bone-growth stimulators, glucose monitors, defibrillators, and other implantable and external devices [8]. It is believed that performance characteristics of Li/CF_x technology are superior to other primary lithium battery chemistries.

Since a lithium anode can be coupled with a variety of different cathode and electrolyte materials, many other combinations other than Li/CF_x lead the market today in primary lithium batteries: Lithium/Manganese Dioxide [9]; Lithium/Sulfur Dioxide [10], Lithium/Thionyl Chloride [11], and Lithium/Polycarbon Monofluoride [12]. The fact that all these different types of primary lithium batteries continue to exist indicates that each one has compelling advantages as well as limitations. For example, Sulfur Dioxide and Thionyl Chloride have relatively high energy and power densities, along with wide operating temperature ranges, but suffer from safety and environmental concerns that make them unsuitable for many applications. Manganese dioxide and polycarbon monofluoride are safe and relatively benign environmentally, but fail to pack the power demanded by some applications.

The advanced Lithium/Carbon Fluoride (Li/CF_x) battery maintains the benefits of high energy and power densities, wide operating temperature range, and long shelf life found in Sulfur Dioxide and Thionyl Chloride batteries, while also employing a solid cathode (with no heavy metals or other toxic materials) to eliminate the safety and environmental concerns. In addition, the advanced CF_x battery possesses none of the operational problems such as passivation exhibited by some other batteries.

Recently, it has been reported that subfluorinated CF_x materials where $0.3 < x < 0.66$ are capable of supporting discharge rates as high as 5C at room temperature with excellent utilization [11]. Another major advantage of the advanced CF_x battery is its ability to exceed all others in both power density and maximum safe current draw. Laboratory tests have demonstrated up to an eight times improvement in high-current applications, and a nearly two times improvement in low-current applications. These properties make the advanced CF_x battery particularly well-suited for applications that require high sustained or pulse currents. Multiwalled Carbon nanotubes (MWNTs) are candidate material of choice for the use in batteries due to their unique electrical and mechanical properties, such as excellent electrical conductivity at room temperature and high aspect ratio. Despite the success of lithium/carbon fluoride (Li/CF_x) on conventional batteries, they do not perform well under high rate conditions, exhibit performance loss in low temperature operation, and are more costly than competing primary lithium chemistries. Use of a low temperature fluorination process and selection of MWNTs as the carbon material, compared to conventional usage of coke, utilize less fluorine (sub fluorinate) to improve performance and conductivity, including both power and rate capabilities. Also, the use multi-walled carbon nanotube offers increased surface area to achieve better rate capabilities as well as improved conductivity. Conventional manufacturing of CF_x cathode material involves use of F_2 gas at high temperatures. F_2 is highly toxic, corrosive, and can cause ignition of organic material on contact. Another alternative technique utilizes HF acid under ambient condition, but does little to reduce risk since HF is also highly corrosive and dangerous to handle. The second approach is to mix the CF_x-based materials with other cathode materials such as MnO_2 [13], SVO [14], SnO_2 [15], and MoO3 to develop a hybrid structure, but the progress in this area is limited without significant improvement on the rate performance.

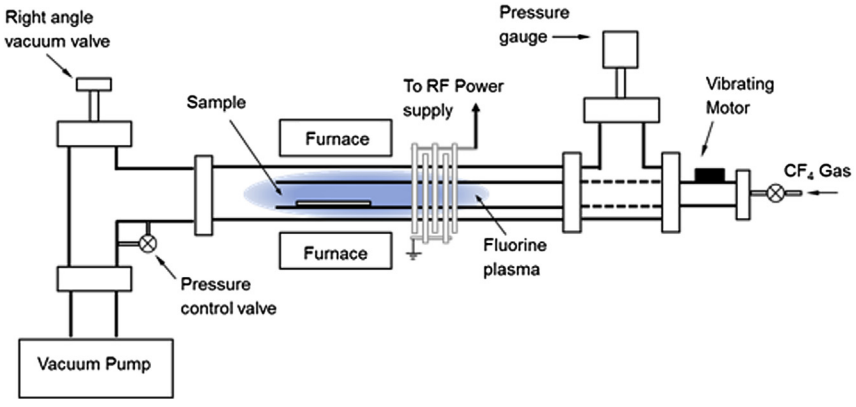

Fig. 2. (a) Schematic diagram of fluorination chamber.

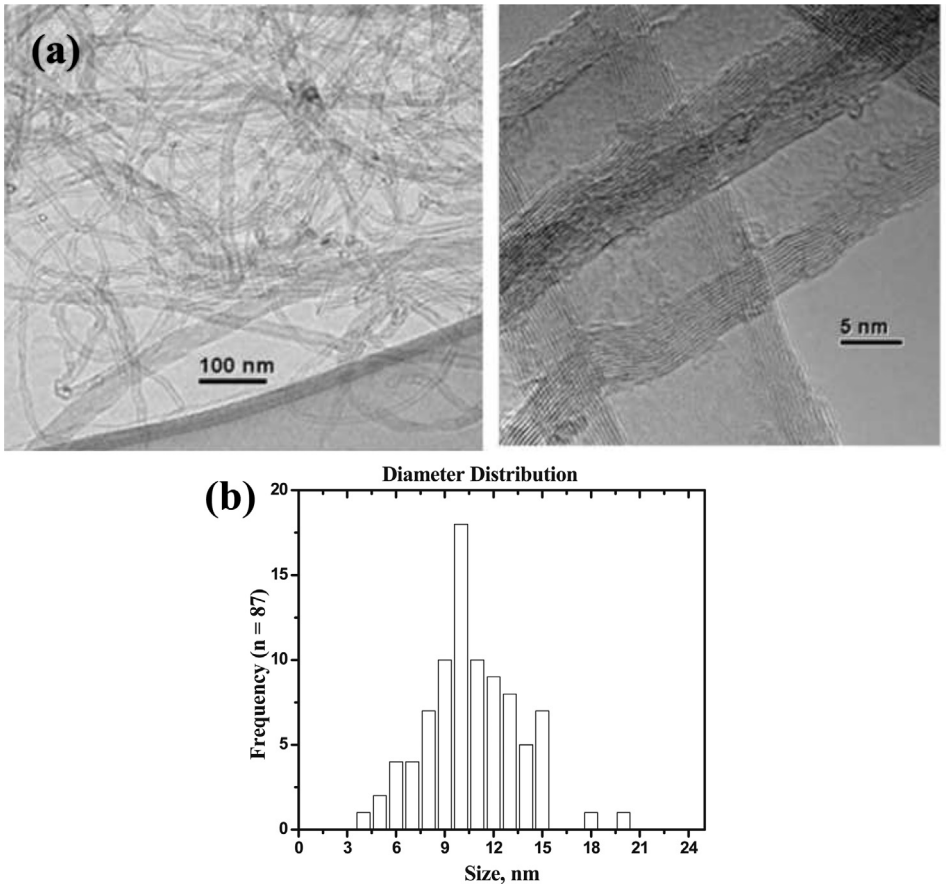

Fig. 3. TEM image of MWNTs after fluorination (b) Diameter distribution of MWCNTs.

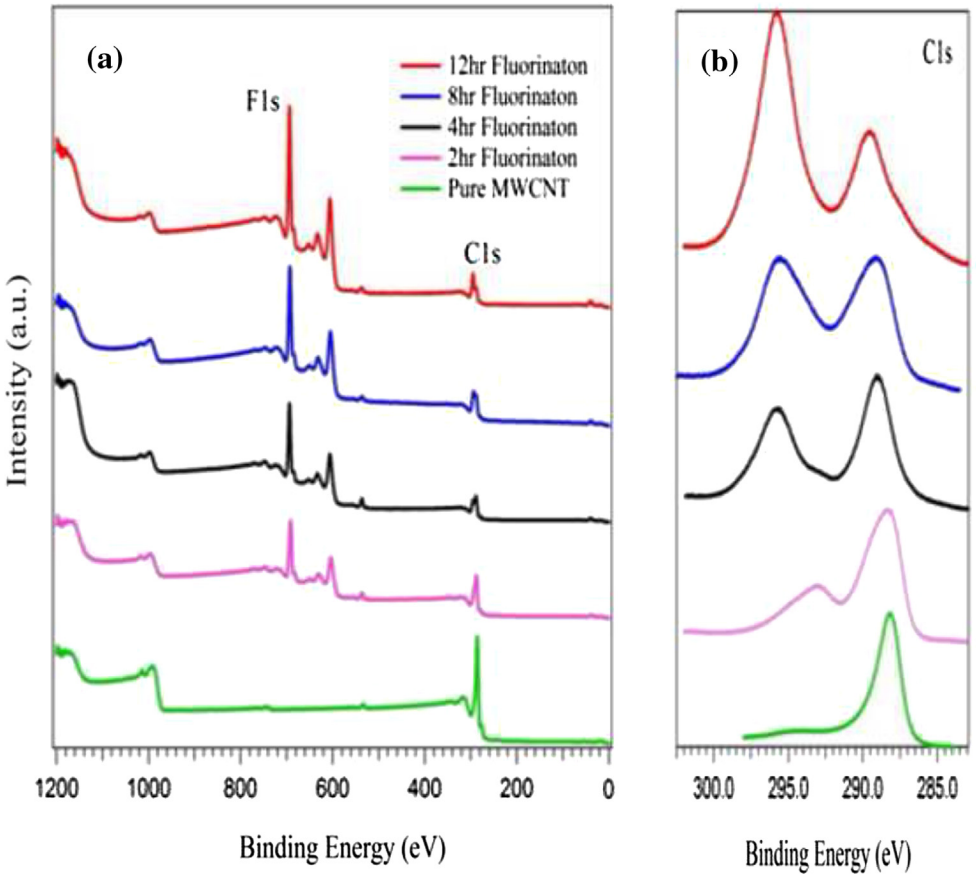

Fig. 4. (a) XPS full scan showing both F1s and C1s peaks for pristine and progressively fluorinated MWNTs (b) detailed features for C1s peak.

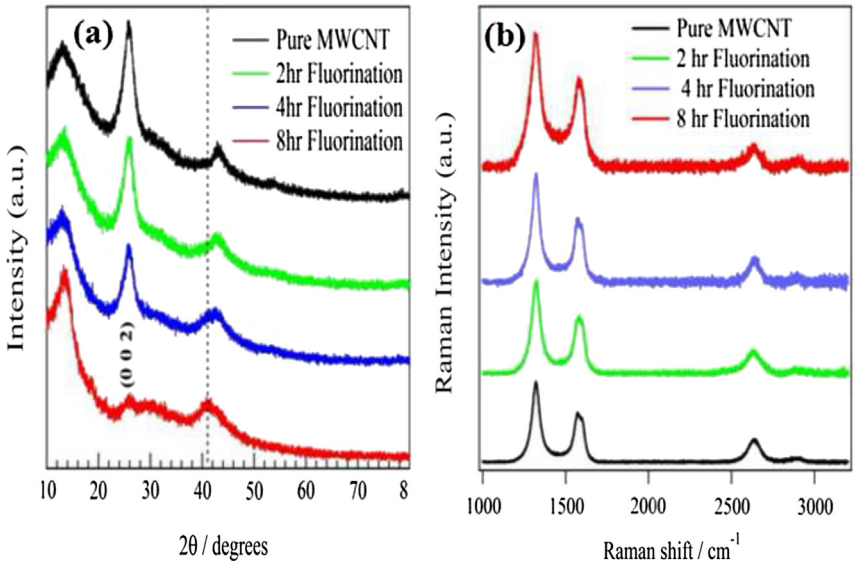

Fig. 5. (a) X-ray Diffraction (b) Raman spectroscopy results for pristine and progressively fluorinated MWNTs.

2. Experimental

2.1. Primary battery (CF_x cathode)

CF_x was used as the active cathode material. A CF_x electrode film was prepared by coating a slurry composed of 85% CF_x, 10% carbon black, and 5% poly (vinylidene fluoride-co-hexafluoropropylene) in *N*-methylpyrrolidone solvent onto a Al foil. The coating was dried in an 80 °C oven to evaporate solvent, and the resulting electrode film was punched into small disks with a diameter of 2 cm^2 for test in button cells for electrochemical cells. The Li metal was used as an anode electrode. The shaped electrode pieces were further dried at 100 °C under vacuum for 8 h, and then transferred to a glove-box for cell assembly. In the glove-box, Li/CF_x button cells were assembled for discharge tests by using a 0.5 mL 1 M $LiPF_6$ solution in a 1:2 (weight) mixture of ethylene carbonate (PC) and dimethyl carbonate (DMC) as the electrolyte and a glass fiber filter (GB-100R) membrane as the separator. Discharge tests were performed on an Arbin battery cycler. In all discharge tests, the cutoff voltage was set at 1.5 V.

2.2. Secondary battery (CF_x anode)

The electrode materials for the anode were prepared using 90 wt% active materials with 2 wt% AB (acetylene black) and 8% PVDF binder in NMP. The well-mixed slurry was coated onto a copper foil using the doctor blade method. The electrode was dried at 180 °C for 3 h under vacuum. The electrochemical characterizations were carried out by using CR-2032 coin-type cells. The coin cell assembling was performed in a glove-box filled with argon (dew point, lower than −80 °C). The negative electrodes were separated by glass fiber filter and the amount of the electrolyte was ca. 0.5 mL. The electrolyte was 1 M $LiPF_6$-EC:DMC (1:2 by volume). The charge–discharge performance was carried out in the voltage range of 3.0–0.005 V at the current density of 100 mA g^{-1}. The cyclic voltammetry measurement of the cell was carried out using eChem software at the voltage range of 3.0–0.005 V with scan speed of 5 mV s^{-1}. The C-rate of the cell was performed at different current densities of 100, 200, 500, 1000, and 1500 mA g^{-1}. Examination of the discharged electrode involves disassembly of the cell in a controlled argon atmosphere glove box, rinsing the electrode with dimethyl carbonate, removing the solvent under vacuum, and then placing the electrode in an air tight holder.

Table 1
The surface texture of MWCNT and NCG before, and after 2 h fluorinations.

Sample	BET surface area (m^2 g^{-1})	Pore volume (cm^3 g^{-1})	Pore size (nm)
MWCNT	240	0.97	14.0
2HF MWCNT	215.8	0.811	13.5
NCG	4.54	0.026	17.2
2HF NCG	6.6	0.021	15.2

3. Results and discussions

3.1. Synthesis of MWNTS

MWNTs were synthesized in large quantity using fluidized bed chemical vapor deposition technique. Fig. 1 shows the SEM image of MWNTs showing high quality pure nanotubes free of catalyst particles and other carbonaceous residues. The diameter distribution of the nanotubes shows average diameter to be ~ 10 nm.

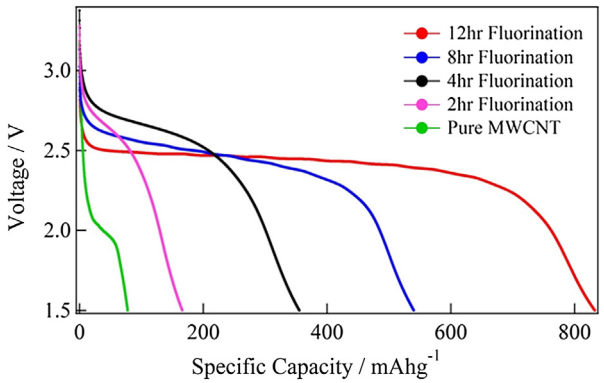

Fig. 6. First discharge capacity curves of CF_x lithium primary battery.

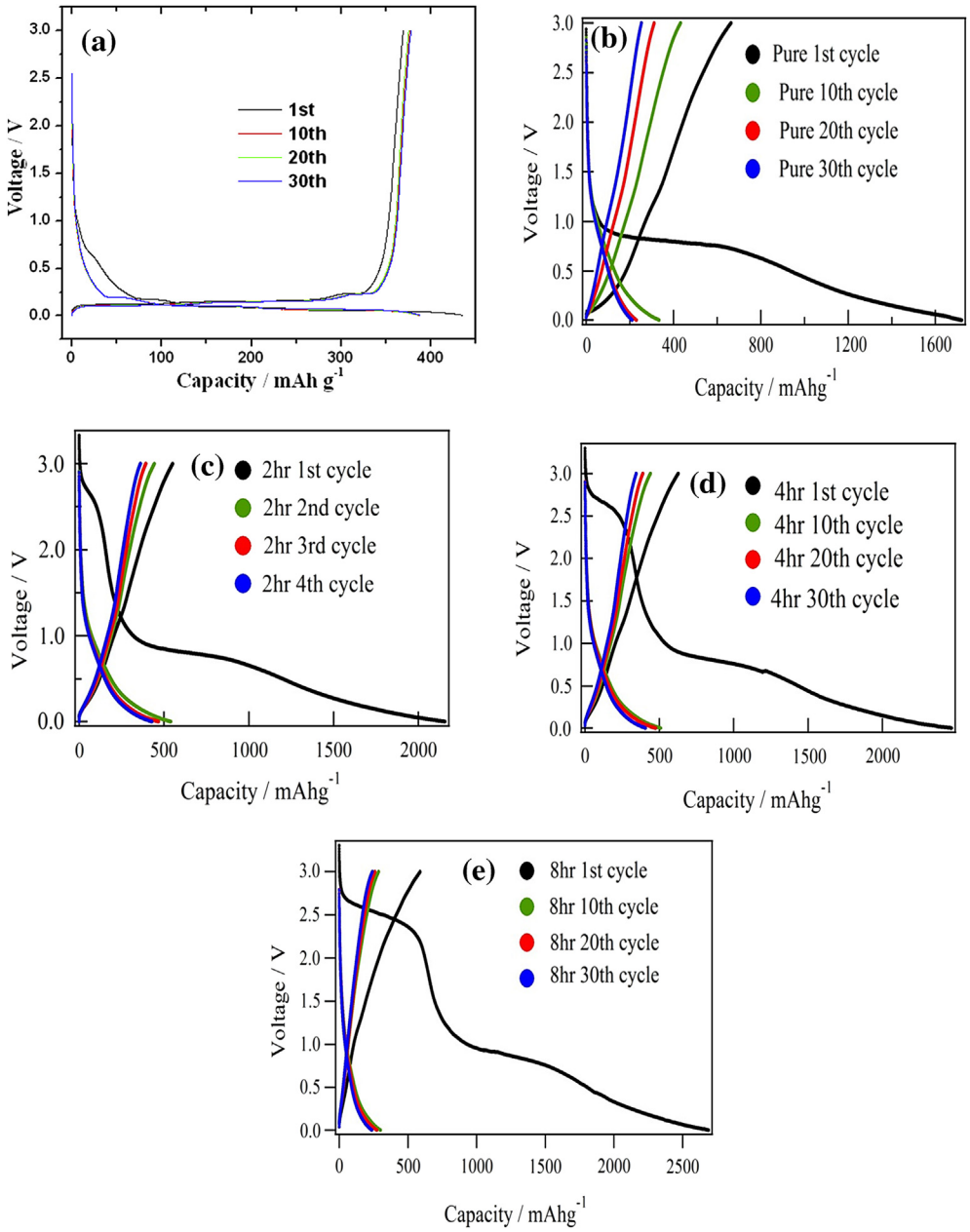

Fig. 7. Discharge and charge profiles of the (a) pure (b) 2 h (c) 4 h, and (d) 8 h MWCNTs obtained after one, ten, twenty and thirty cycles.

3.2. Fluorination of MWNTs

A custom-designed, split ring, capacitively coupled RF (radio frequency) plasma system (13.56 MHz, Max. power 600 W) was utilized for fluorination of MWNTs. MWNTs were loaded into a quartz boat, and CF4 gas was introduced at controlled flow rates and pressure. Fig. 2 shows plasma functionalization setup. CF_4 gas was supplied to the system at a 10 sccm flow rate and chamber pressure was maintained at 5 torr. Sample is heated up to 150 °C. This reactor consisted of a sample vibrator attached to the sample holder. The vibrator was utilized to shake the sample holder during the functionalization process. This will facilitate homogeneous fluorination and significantly cut down the functionalization time.

As seen in the SEM images (Fig. 3a) it is evident that the MWNTs are larger in diameter and better dispersed as a result of fluorination. TEM images Fig. 3b confirm that even after intense fluorination process, MWNTs retain their structural integrity. The Fluorination was characterized using XPS (X-ray photo emission spectroscopy) and EDAX (energy dispersed X-ray spectroscopy). TEM images confirm that even after intense fluorination process, MWNTs retain their structural integrity. The Fluorination was characterized using XPS (X-ray photo emission spectroscopy) and EDAX (energy dispersed X-ray spectroscopy).

3.3. Characterization of fluorinated MWCNTs

The pristine MWCNTs and fluorinated MWCNTs were characterized by field emission scanning electron microscopy (FE-SEM) (FEI Nova600), X-ray diffraction (XRD) (Bruker D8 Discover), and transmission electron microscopy (TEM) (Tecnai F20 FEITEM with a Gatan 2002 GIF system). Raman spectroscopy of the samples was studied (in-Via Renishaw micro-Raman system with a cooled CCD

detector) with a He–Ne laser (632.8 nm) as an excitation source. The BET surface area was determined by the nitrogen adsorption/desorption data obtained using the Micromeretics TriStar 3000.

The XPS spectra of the MWCNTs used in this study were obtained with a MultiLab 3000 spectrometer (Thermo electron corporation, England). The spectra were analyzed in order to study the nature of chemical species on the surface of MWCNTs after fluorination using Al Kα (1485.6 eV) X-ray, produced at 14.9 keV of anode voltage. All measurements were obtained at 10^{-9} Torr chamber pressure. XPS survey graphs of pure and fluorinated MWCNT samples are plotted in Fig. 4a. All spectra show distinct carbon and oxygen peaks around 285.0 eV and 533.0 eV respectively. Fluorine peaks were also found around 687.7 eV on fluorinated MWCNTs. It is clear from the plot that the intensity of the C1s peak decreases while that of F1s peak increases as the fluorination progresses.

Fig. 4b shows the detailed features for C1s peak. For C1s spectra, the peak at a binding energy (284.6 eV) is assigned to sp^2 hybridized C atoms in MWCNT. Another peak at higher binding energy (289.4 eV) is assigned to sp^3 hybridized C atoms due to the formation of C–F bonds as a result of fluorination. The first peak (sp^2) is seen to weaken while the second peak (sp^3) strengthens as the fluorination progresses. Based on EDAX data, the four samples have been identified as $CF_{0.04}$, $CF_{0.26}$, $CF_{0.56}$, and CF_1.

X-ray diffraction patterns of fluorinated samples are shown in Fig. 5a. The X-ray pattern of the MWCNT displays the presence of two peaks at 25.80° (3.47 Å) and 42.75° (2.12 Å) assigned to (002) and (100) diffractions corresponding to the interlayer spacing (0.34 nm) of the nanotube in good agreement with that of the previous literature [14]. It is clear that fluorination reduces intensity of (002) peak of carbon nanotubes. The intensity of this peak increases with the degree of fluorination. This peak is evident for the non-destructed structure of MWCNT. However, the absence of peak corresponding to peak (002) in fully fluorinated sample implies that excessive fluorination destroys graphite-like structure of pristine MWCNT. Fluorination affects only the first few layers of the MWCNTs, resulting in increased interlayer distances. With excessive fluorination, these layers separate from the parent tube and therefore no longer have graphite-like structure.

The BET surface area of MWCNT, and NCG before and after fluorination was determined by the nitrogen adsorption/desorption data obtained using the Micromeretics TriStar 3000. The BET surface area of MWCNT before fluorination is 240 $m^2\ g^{-1}$ with pore volume and pore size of 0.97 $cm^3\ g^{-1}$ and 14.0 nm respectively. After 2 h fluorination, the BET surface area of MWCNT was reduced to 215.8 $m^2\ g^{-1}$ with pore volume of ca. 0.811 $cm^3\ g^{-1}$, and pore size of 13.5 nm respectively. The BET surface area of NCG (Natural Chinese graphite) before fluorination is 4.54 $m^2\ g^{-1}$ with pore volume of 0.026 $cm^3\ g^{-1}$, and pore size diameter of 17.2 nm. After 2 h fluorination, The BET surface area of NCG was increased to 6.6 $m^2\ g^{-1}$ with pore volume of 0.021 $cm^3\ g^{-1}$, and pore size of 15.2 nm respectively as shown in Table 1.

Fig. 5b shows the Raman spectra of pristine and progressively fluorinated MWNTs acquired using a Renishaw Invia Raman spectrometer with 632 nm excitation. The characteristic D, G, and 2D bands are seen in all 3 samples. As fluorination progresses, the ratio between D and G bands is seen to increase as F atoms are incorporated into the sp^2 carbon lattice.

3.4. Primary battery (Li/CF_x) performance

The results for pristine, partially fluorinated, and fully fluorinated MWNTs are shown in Fig. 6. The first 4-cycle discharge capacity is seen to increase as fluorination progresses. Pristine MWNTs show only 80 mAh g^{-1} specific capacity (first cycle discharge), but it increases to 180, 380, 550, and finally to 830 mAh g^{-1} as fluorination progresses.

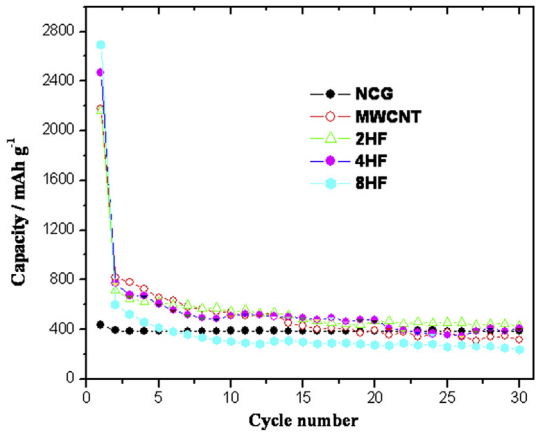

Fig. 8. Cycling stability of the MWCNT with different fluorine concentration.

Fig. 7a, b, c, d and e show the discharge and charge profiles for NCG (Natural Chinese graphite), MWCNTs with different concentrations of fluorine obtained after one, ten, twenty, and thirty cycles. First columbic efficiency is associated with the irreversible capacity loss in the 1st cycle. This process involves electrolyte decomposition and subsequent formation of surface film called solid electrolyte interface (SEI) on anode. Some of the lithium ions are consumed during the formation of SEI, and therefore are not inserted in MWCNT surface. This is one of the challenges of developing carbonaceous anodes. Good anode material should suppress the electrochemical decomposition of solvents for the formation of SEI. Since electrochemical reactions take place at the surface of electrodes, surface structure is an important factor determining the electrochemical characteristics of carbon materials.

The 8 h fluorination shows a lower 1st cycle discharge capacity. This particular behavior may be related to the fluorine-induced disorder of the MWCNT structure. The cathode reduction of fluorinated MWCNT is limited by the lithium ion's diffusion within the multi-tubes structure. Mild fluorinated MWCNT has less structure damages. Therefore, lithium diffusion is hindered by low defect density. For highly fluorinated MWCNT, additional intercalated

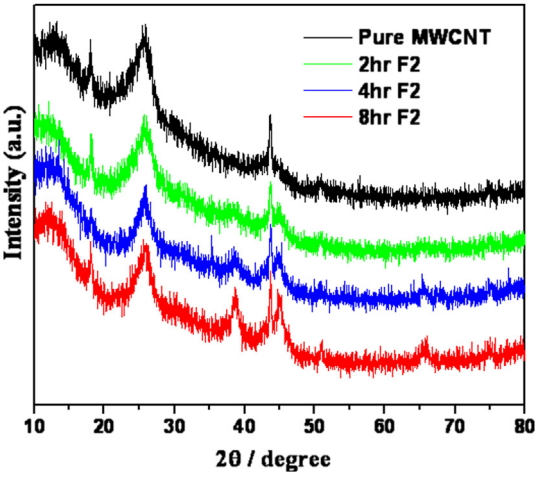

Fig. 9. Ex-situ XRD for pristine and fluorinated MWNTs electrodes after first cycle discharge.

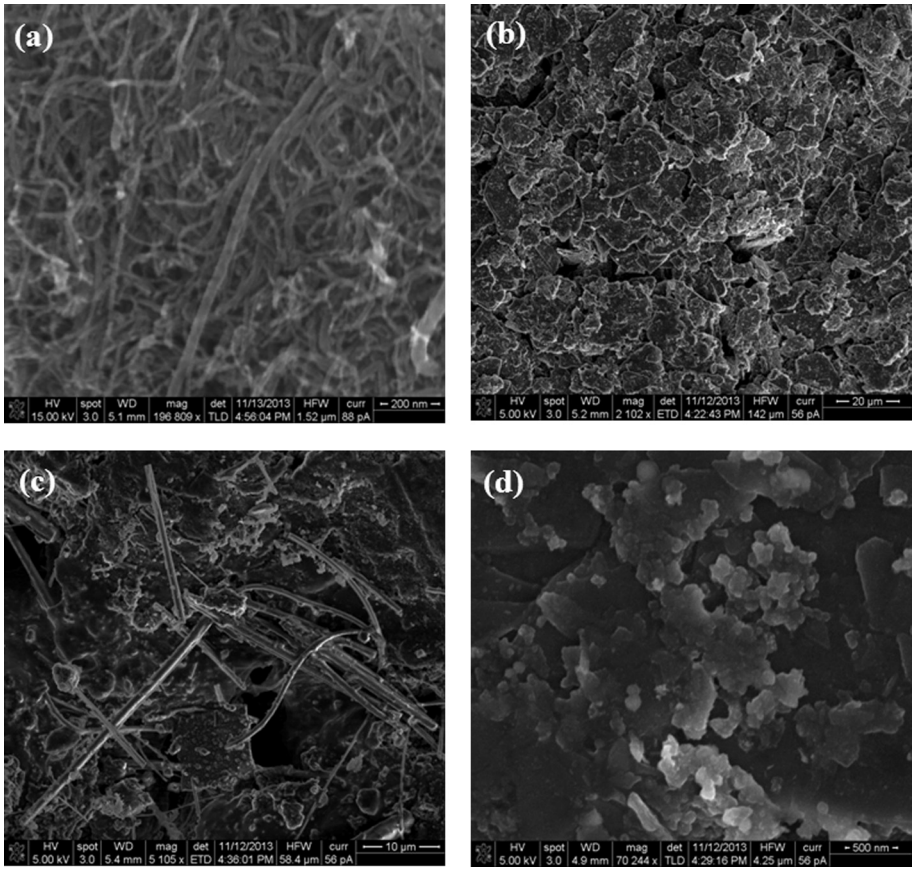

Fig. 10. SEM images of 2 h fluorinated (a) MWCNT and (b) Natural graphite (NCG) electrodes surface before discharge and (c) MWCNT, and (d) NCG electrodes after discharge to 0.005 V.

fluorine creates more strains for their accommodation. This will lead to increased defect density. Defects such as cracks in the carbon layers and opening of the nanotube ends are additional paths for lithium ions to diffuse within the core of the fluorinated structure and to access the electrochemically active C–F sites. The presence of the non-fluorinated carbons in the fluorinated MWCNT core, even in small amounts, favors higher electron flow and accordingly enhances the electrode reaction kinetics.

We tested the samples for Li-ion secondary battery performance using CF_x based on MWNTs as the anode electrode and compared with that of common NCG as shown in Fig. 8. The capacity was determined when they were discharged/charged for 30 cycles between the voltage range of 3 V and 0.005 V. Fully fluorinated sample shows low rechargeable capacity compared to the sub-fluorinated samples. Preliminary results show that mildly fluorinated (2 h) MWNTs show high capacity ~713 mAh g^{-1} during initial cycle and shows stable cycleability of 429 mAh g^{-1} after 30 cycles. It shows ~ 60.2% capacity retention over 30 cycles. But

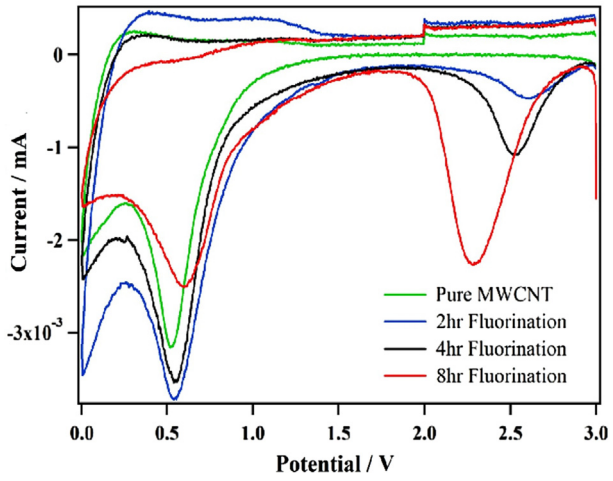

Fig. 11. Cyclic voltammograms for the 1st cycle of pure and plasma fluorinated MWCNT.

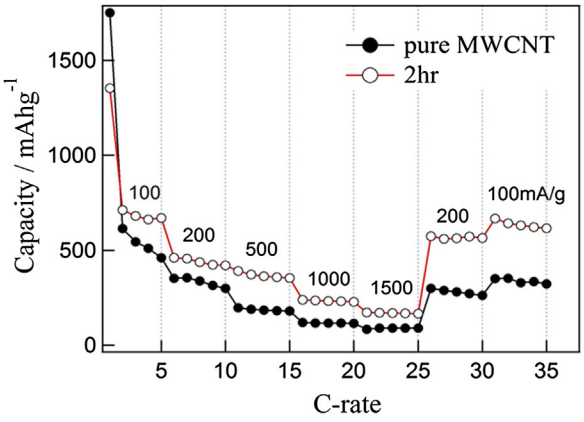

Fig. 12. Capacities vs. cycle number of MWCNT and 2 h fluorinated MWCNT at current densities of 200 mA g^{-1}, 500 mA g^{-1}, 1000 mA g^{-1}, and 1.5 A g^{-1}.

pristine MWCNT shows starting capacity of ~650 mAh g^{-1}, with retention capacity of ~150 mAh g^{-1} after 30 cycles. Pure MWCNT shows ~ 23% capacity retention over 30 cycles. The 4 h and 8 h MWCNT shows capacities ~ 771 and 596 mAh g^{-1} during the initial cycle, and after 30 cycles they still retain the capacities of 407 and 238 mAh g^{-1}. The capacity retention rates of 4 h and 8 h fluorinated MWCNT were 52.8% and 39.9% respectively. NCG electrode shows initial capacity of ~435 mAh g^{-1}, with stable capacity of ~388 mAh g^{-1} after 30 cycles. Several coin cells with different fluorine concentrations were tested. The 2 h fluorination exhibited similar high initial capacities, good cycle stabilities, and excellent capacity retentions at high rates.

Fig. 9 shows *ex-situ* XRD data for pristine and progressively fluorinated MWNTs after first discharge cycle. The C(200) XRD peak (~25^0) is seen to gradually broaden as a result of lithiation. The new peaks appearing at 45^0 and 66^0 correspond to LiF as a result of lithiation leading to $CF_x + Li \rightarrow LiF + C$.

The SEM images of fluorinated MWCNT and NCG electrodes before discharge are shown in Fig. 10a, and (b). After discharge to 0.005 V, it is clear from the SEM images that the fluorinated MWCNT and NCG electrodes were completely covered with SEI (solid electrolyte interface) film with a morphology that is quite different as shown in Fig. 10c, and (d).

Fig. 11 shows the cyclic voltammograms obtained for pure and fluorinated MWCNT. A large cathodic current peak was found at 0.6 V. This is an indication of the electrochemical reduction of electrolyte and subsequent formation of solid electrolyte interface (SEI). Higher fluorine concentration will reduce this peak, implying that SEI is formed by the decomposition of less amounts of electrolyte. Another large cathodic peak shows up at ~2.6 V. This cathodic peak was enhanced and shifted with increasing plasma-treatment time as shown in Fig. 11.

The 2 h fluorinated MWCNT also has excellent rate performance. Fig. 12 shows that the capacity at 100 mA g^{-1} current density is 712 mAh g^{-1} and 172 mAh g^{-1} at 1.5A g^{-1}. The capacity retention is ~80% after testing for 35 cycles. Five formation cycles at 100 mA g^{-1}, 5 cycles each at current densities of 200 mA g^{-1}, 500 mA g^{-1}, 1000 mA g^{-1}, and 1.5 A g^{-1}. This demonstrates the recovery of the mild fluorinated MWCNT after subjecting it to different charge–discharge rates.

4. Conclusions

Fluorine functionalization setup was further modified to prepare CF_x battery electrode materials. Fully fluorinated MWCNT shows low rechargeable capacity compared to the subfluorinated samples. Mildly fluorinated (2 h) MWNTs show high capacity and show better stability during charge discharge cycles. High concentrations of fluorine seem to negatively affect capacity retention due to the increased defect densities, while these defects of nanotubes will provide additional paths for lithium ions to diffuse within the core of the fluorinated structure and to access the electrochemically active C–F sites. So, the first cycle discharge capacity is seen to increase as the fluorination progresses. Finally, controllably fluorinated carbon nanotubes showed promise for high capacity primary and secondary battery performances.

Acknowledgments

This project was partially supported by the grant from the Perm Ministry of Education, Grant No. C-26/628.

Appendix A. Supplementary material

Supplementary data related to this article can be found at http://dx.doi.org/10.1016/j.jpowsour.2013.12.076.

References

[1] D. Linden, T.B. Reddy, Handbook of Batteries, McGraw-Hill, 2002.
[2] J. Read, et al., Performance Evaluation of Commercial CF_x Materials in Lithium Batteries, 2009. DTIC Document.
[3] T. Tan, K. Lam, H. Yumoto, in: Meeting Abstracts, 2006. The Electrochemical Society.
[4] K. Chen, D.R. Merrit, W.G. Howard, C.L. Schmidt, P.M. Skarskad, J. Power Sources 162 (2006) 837–840.
[5] Y. Liu, X. Zhou, Y. Guo, J. Power Sources 184 (2008) 303–307.
[6] T. Nakajima, N. Watanabe, Graphite Fluorides and Carbon–Fluorine Compounds, CRC Press, Boca Raton, FL, 1991.
[7] W. Greatbatch, C.F. Holmes, E.S. Takeuchi, S.J. Ebel, Pacing Clin. Electrophysiol. 19 (1996) 1836–1840.
[8] S.S. Zhang, D. Foster, J. Read, J. Power Sources 2009 (188) (2009) 532–537.
[9] B. Ratnakumar, et al., J. Electrochem. Soc. 154 (2007) A715–A724.
[10] D.J. Klionsky, et al., Autophagy 8 (2012) 445–544.
[11] J. Whitacre, R. Yamazi, A. Hamwi, M.C. Smart, W. Bennett, G.K. Surya Prakash, T. Miller, R.K. Bugga, J. Power Sources 160 (2006) 577–584.
[12] Z. Zhang, J. Peng, H. Zhang, Appl. Phys. Lett. 79 (2001) 3515–3517.
[13] Z. Wang, J. Wang, Z. Li, P. Gong, X. Liu, L. Zhang, J. Ren, H. Wang, S. Yang, Carbon 50 (2012) 5403–5410.
[14] Y. Saito, T. Yoshikawa, S. Bandow, M. Tomita, T. Hayashi, Phys. Rev. B 48 (1993) 1907–1909.
[15] X.W. Guo, X.P. Fang, Y. Sun, L.Y. Shen, Z.X. Wang, L.Q. Chen, J. Power Sources 226 (2013) 75–81.